Remote Sensing Mapping of Turbidity in the Upper San Francisco Estuary

Francine Mejia, Geography 342

Introduction

The sensitivity of reflectance to sediment, chlorophyll a, and colored DOM (CDOM) in the visible and near-infrared wavelengths have made remote sensing a great tool to measure turbidity and other water quality parameters concentrations. Remote sensing can be used to obtain either qualitative or quantitative estimates and numerous studies have been published on this subject (Moore 1980, Fraser 1998, Gitelson et al. 2000, Chen et al. 2007, Ramakrishna et al. 2007, Sun et al. 2011). Matthews (2011) provided a thorough review of empirical algorithms for quantitatively estimating chlorophyll a and total suspended solids (TSS) among other parameters from remote sensors (space/air borne and in situ remote sensors) in inland and transitional waters. Matthews (2011) also identified bands, band ratios and band arithmetic algorithms to use in inland and transitional waters.

The main purpose of this project is to determine whether remote sensing is a good tool to supplement turbidity and TSS monitoring in the San Francisco estuary. The California Department of Water Resources routinely sample different regions of the estuary. However, ground sampling is costly, does not extend to all regions of the estuary and is measured at discrete locations. Remote sensing would allow continuous coverage as well as comparison between regions of the estuary. This project allowed us to develop a procedure to map and monitor the spatial and temporal distribution of turbidity, and total suspended solids.

Methods and Results

Suspended sediment concentrations, nephelometric turbidity and chlorophyll a concentrations collected along the San Joaquin and Sacramento Rivers by the California Department of Water Resources Monitoring Program (Figure 1) were compared to Landsat imagery (Thematic Mapper; Landsat 5) obtained from the Earthexplorer USGS website (Figure 2). (http://edcsns17.cr.usgs.gov/NewEarthExplorer/). Field data (Ground samples) were collected on July 26, 2010, August 12-13 and August 26-27, 2010. Landsat 5 data has a temporal resolution of 16 days. Landsat imagery for the San Francisco estuary that corresponded most closely to our field measurements was available on July 29, 2010, August 14, 2010 and August 30, 2010. For the class project I focused on the July 2010 data in the San Joaquin River (Figure 1).

Reflectance data for each site was also collected along with the water quality parameters. UC Davis was responsible for this portion of the data collection. Remote sensing surface reflectance was measured using an Analytic Systems Device (ASD) field spectroradiometer, which measures reflected light from 0.35-2.5 μm wavelengths. At each sampling location, the sensor was calibrated using a Spectralon calibration target, and normalized for reflectance. Fifteen measurements were collected at each sampling location. All field remote sensing reflectance measurements were conducted following NASA protocol for water surface remote sensing measurements. All field remote sensing measurements were calibrated from radiance to reflectance using RS3 field spectrometry software. The reflectance data was subset to only include the visible and near-infrared regions (350-1000 nm). The mean reflectance for each sampling location was calculated using SAMS spectral analyst software (CSTARS, UC Davis).

Ramakrishna et al. (2007) suggested data collection and pre-processing scheme was mostly followed:

1. Satellite Image - Suitable Landsat, were chosen to do the analysis.
2. Geo Referencing - Geo-referencing maps the satellite imagery pixels to latitude and longitude values.
3. Ground Truth - Ground Truth samples obtained were +/- 3 days window of the image date for TSS.
4. Water Only Image – Water only image was created by carrying out simple image classification.
5. Morphological Operations - Morphological operations like closing, erosion and mask out sections close to shoreline etc. Pixels which are close to the shore, influenced by presence of vegetation are removed. This step was not carried out. Samples were collected in the main river channel and boat used was too large to collect samples near shoreline.

Below is a step by step description of the data classification and processing carried out for the July 29, 2010 Landsat 5 Imagery:

Step 1. Satellite image was retrieved from the Earth Explorer website. Below is a data set attribute table summarizing image quality information as well as coverage extent for July 26, 2010 satellite image.

Data Set Attribute	Attribute Value
Landsat Scene Identifier	LT50440342010210EDC00
Spacecraft Identifier	LANDSAT_5
Sensor Mode	BUMPER
Station Identifier	EDC
Day Night	DAY
WRS Path	044
WRS Row	034
WRS Type	2
Data Category	NOMINAL
Date Acquired	2010/07/29
Start Time	2010:210:18:36:17.21688
Stop Time	2010:210:18:36:43.82981
Data Type Level 1	TM L1T
Sensor Anomalies	N
Acquisition Quality	9
Quality Band 1	9
Quality Band 2	9
Quality Band 3	9
Quality Band 4	9
Quality Band 5	9
Quality Band 6	9
Quality Band 7	9
Cloud Cover	37.92
Cloud Cover Quadrant Upper Lef	46.45
Cloud Cover Quadrant Upper Rig	.01
Cloud Cover Quadrant Lower Lef	88.74
Cloud Cover Quadrant Lower Rig	16.49
Sun Elevation	61.39925229
Sun Azimuth	124.41131752
Scene Center Latitude	37.48142 (37°28'53.11"N)
Scene Center Longitude	-122.12600 (122°07'33.60"W)
Corner Upper Left Latitude	38.41676 (38°25'00.34"N)
Corner Upper Left Longitude	-122.92961 (122°55'46.60"W)
Corner Upper Right Latitude	38.11407 (38°06'50.65"N)
Corner Upper Right Longitude	-120.85091 (120°51'03.28"W)

Corner Lower Left Latitude	36.83634 (36°50'10.82"N)
Corner Lower Left Longitude	-123.38058 (123°22'50.09"W)
Corner Lower Right Latitude	36.53982 (36°32'23.35"N)
Corner Lower Right Longitude	-121.34351 (121°20'36.64"W)
Browse Exists	Yes

Step 2. July 29, 2010 image was geo-referenced using the Transverse Mercator WGS 84 UTM Zone 10N projection. All the bands for the image were composited into one (Figure 1).

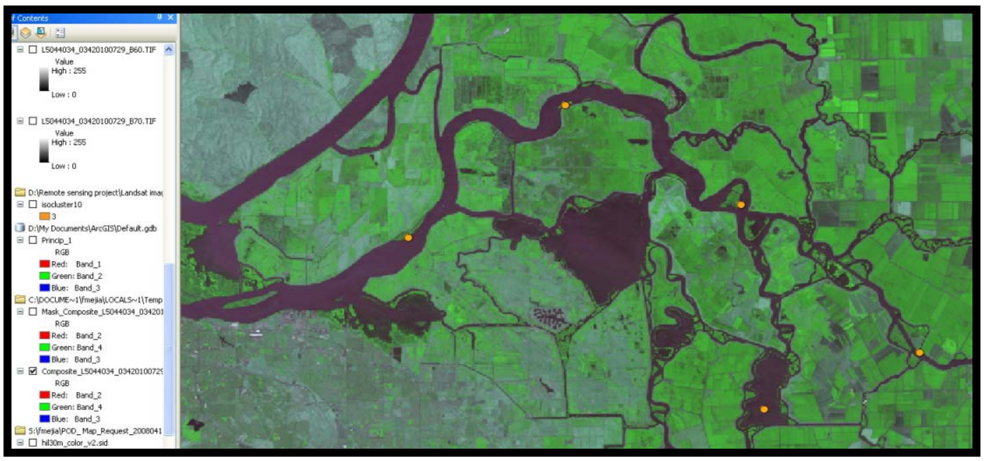

Figure 1. Landsat 5 imagery from July 29, 2010. Orange circles indicate discrete sampling locations where TSS samples were collected.

Step 3. An unsupervised classification was run using the Isocluster unsupervised classification method from the ArcGIS 10.0 Image analysis tool. 10 classes or categories were selected (Figure 2).

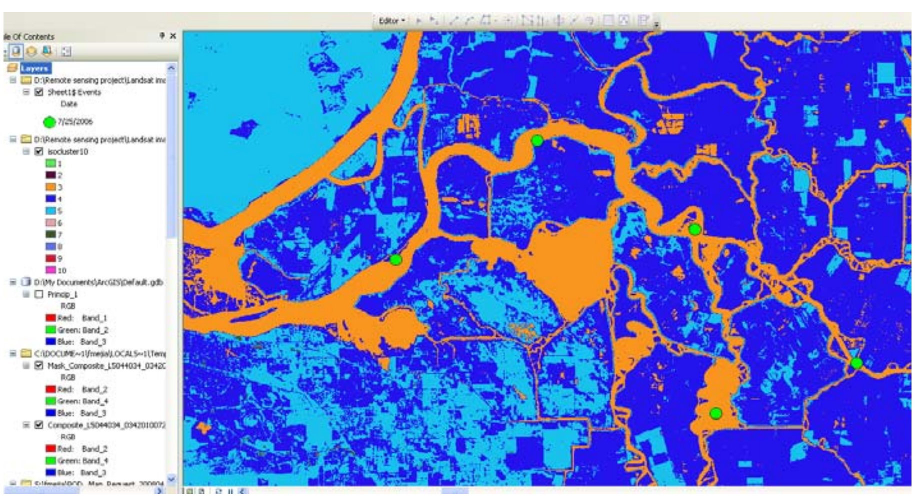

Figure 2 Results from the unsupervised classification. All 10 classes are shown.

Step 4. Class 3 seemed to appropriately categorize water, so this class was isolated. The main purpose for isolating this category was so a supervised classification could be run with the training sites created from the sample locations visited in July 26, 2010 (Figure 3).

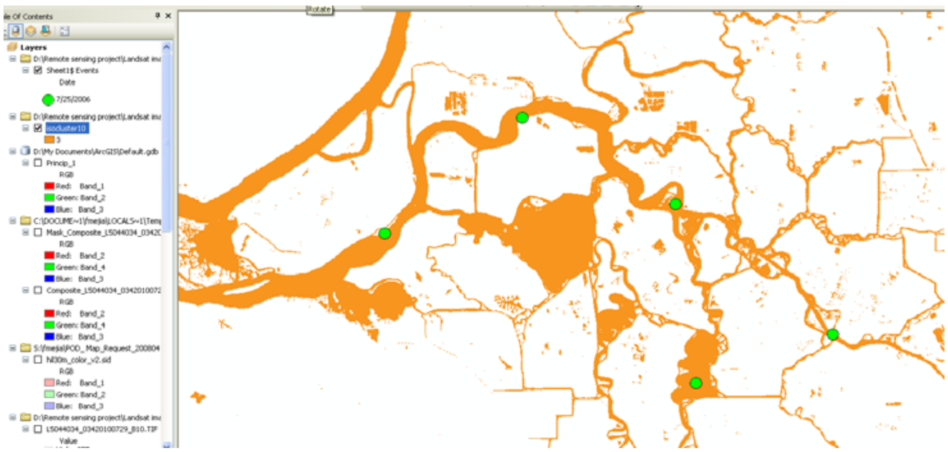

Figure 3 Isolated water class.

Step 5. Five training sites were created to obtain mean wavelengths (brilliance) data to develop the relationship between reflectance and TSS. Figure 4 shows the San Joaquin #2 training site polygon. Mildred Island site was excluded from further analysis as it has been previously categorized as an Island site (shallow).

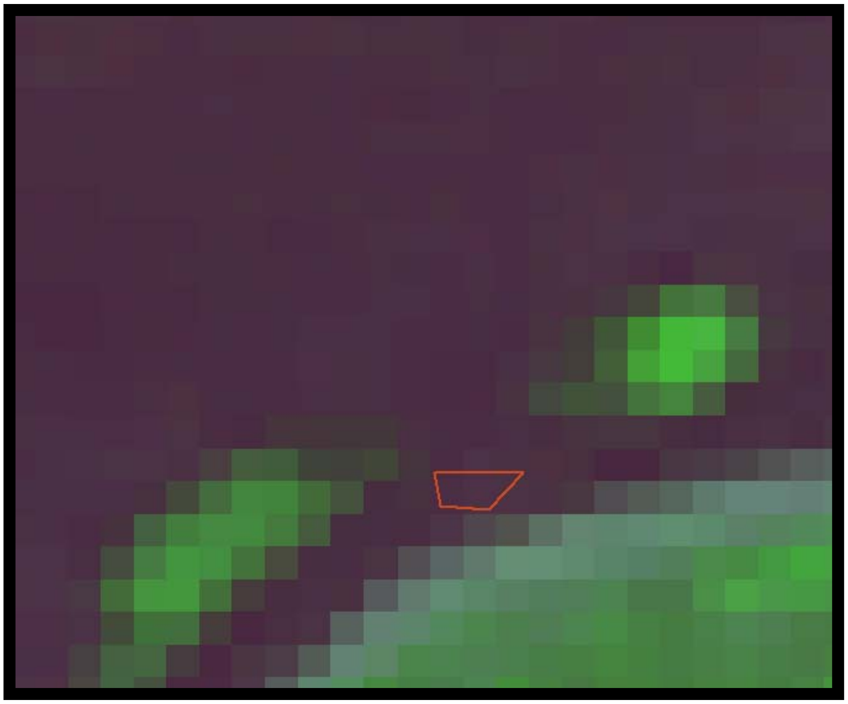

Figure 4. San Joaquin River #2 training site.

The mean brilliance values for each band at each site were used to compare field measurements collected at each site (Table 2).

Table 2 Training sites mean reflectance values (nm).

Sites	Date	Band 1	Band 2	Band 3	Band 4	Band 5	Band 6
		450-520	520-600	630-690	760-900	1550-1750	1040-1250
sjr3_fd	7/25/2006	74.0	34.5	29.0	17.0	17.0	134.0
sjr4_fd	7/25/2006	69.5	29.5	23.5	15.5	14.5	129.5
sjr5_fd	7/25/2006	71.0	30.0	28.0	20.5	19.0	137.5
sjr6_fd	7/25/2006	70.5	29.6	26.2	18.7	18.9	131.3

Step 5. Discrete TSS values were compared to discrete reflectance measurements collected by UC Davis (Figure 5). Wavelengths were grouped to match the Landsat bands. Derivative values were used instead of raw values to improve fit. The first derivative of a spectral reflectivity is defined as its rate of change with respect to wavelength. First derivatives are computed by dividing the difference between successive reflectance values by the wavelength interval separating them (Rundquist et al. 1996). The in situ reflectance values seemed to have a better

relationship between R450 and R520 and between R630 and R690. Both regressions had R^2 around 0.72.

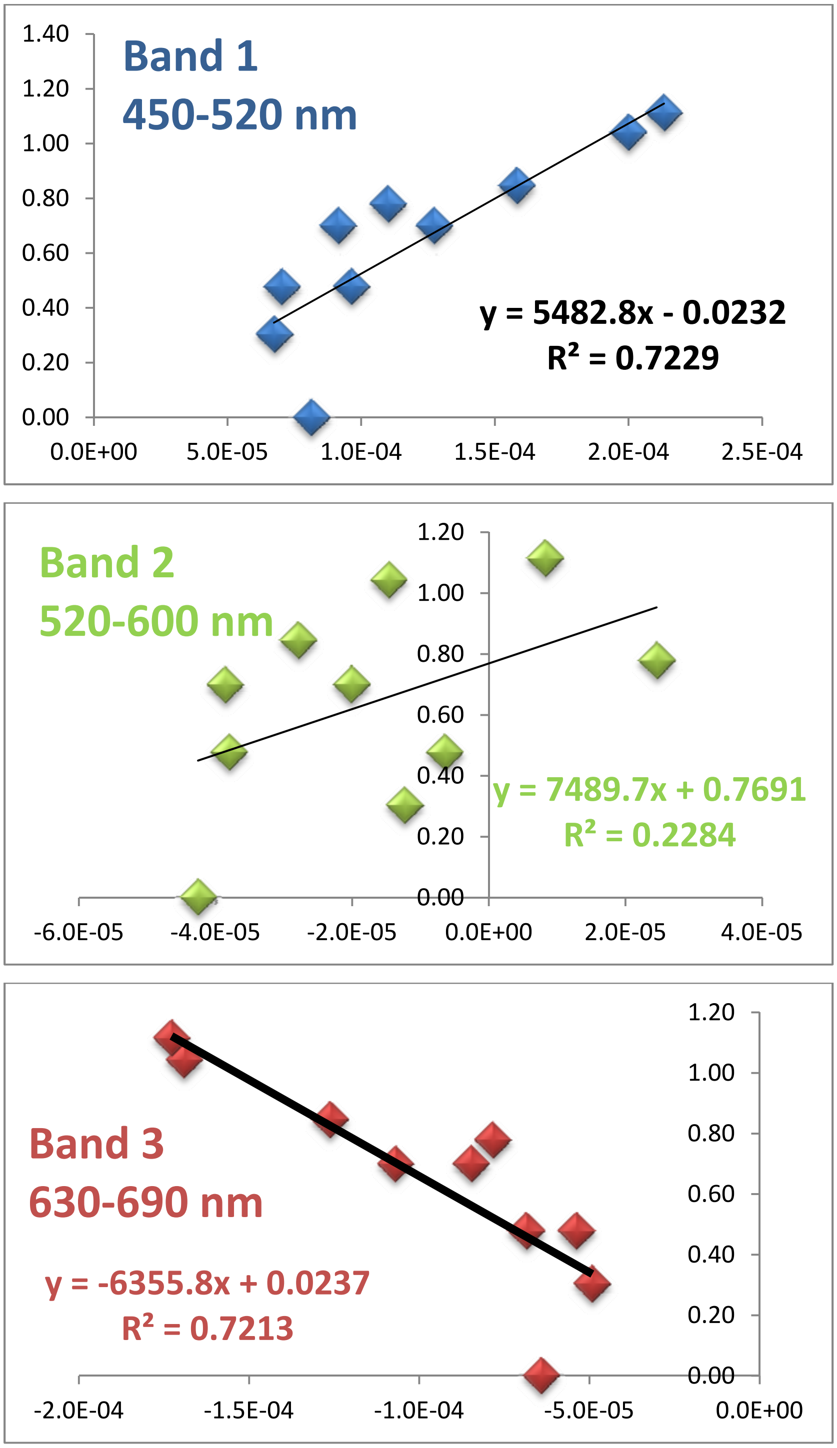

Figure 5. Linear regressions involving TSS mg/l (Y-axis) and reflectance values nm (X-axis).

Step 6. Gitelson et al. (1993) empirical relationship of spectral reflectance and TSS with the greatest correlation coefficient (r=0.93) was used to compare the field TSS measurements with the reflectance data obtained from the Landsat image. Gitelson et al.'s relationship is best described as a difference ratio algorithm (R560-R520)/ (R560+R520). Gitelson et al (1993) suggested using R560 and R520 because R560 is maximally sensitive to variation of suspended solids concentration while R520 is relatively insensitive to variations in the water quality parameters.

This is the final step. Two more images (corresponding additional sampling dates) need to be analyzed to make this relationship more robust. During this second round of analysis additional sites will be added as well.

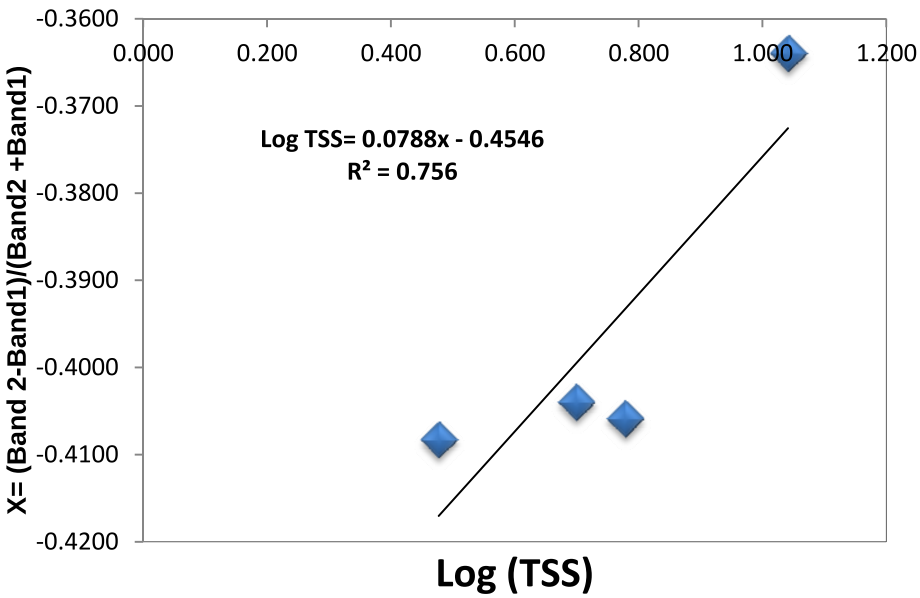

Figure 6. Linear regression involving log TSS values and the difference ratio of Bands 1 and 2 obtained from the Landsat imagery.

Discussion

The two biggest hurdles for this project were 1) getting acquainted with the data already collected by the University of California at Davis remote sensing lab and 2) understanding the scientific literature on the subject as it pertained to correlating turbidity and chlorophyll a to remote sensing data. There is a large amount of data published on this subject and distilling what was pertinent to the project was a difficult task. Figuring out which bands correlate best to turbidity was challenging as there is not agreement among studies on which bands or ratios are best for TSS estimation. The best source was Matthews (2011); it provided a thorough review.

Limitations

Atmospheric effects or the effects of CDOM were not corrected. CDOM effects are usually negligible at wavelengths greater than 550nm (Matthews 2011). However, our peak wavelengths were near 580 nm so CDOM may affect our ability to discriminate the signal from chlorophyll a; main reason why this was not attempted.

As mentioned before sample size was too small (N=4). Although the relationship shows promising results, more sites must be added. This can be accomplished once the other two images are processed and training sites are created.

References:

Chen, Z. , F. E. Muller-Karger, C. Hu. 2007. Remote sensing of water clarity in Tampa Bay. Remote Sensing of Environment 109: 249-259.

Fraser, R.N. 1998. Multispectral remote sensing of turbidity among Nebraska Sand Hills lakes. International Journal of Remote Sensing 19(15): 3011-3016.

Gitelson, A., G. Garbuzov, F. Szilagyi, K-H. Mittenzwey, A.Karnieli, and A. Kaiser. 1993. Quantitative remote sensing methods for real time monitoring of inland waters quality. International Journal of Remote Sensing 14(7): 1269-1295.

Gitelson, A., Y.Z. Yacobi, J.F. Schalles, D.C. Rundquist, L. Han, R. Stark , and D. Etzion. 2000. Archives of Hydrobiologia. Special Issues Advanced Limnology. 55; 121-136.

Matthews, M.W. 2011. A current review of empirical procedures of remote sensing in inland and near-coastal transitional waters. International Journal of Remote Sensing 32(21): 6855-6899.

Moore, G.K. 1980. Satellite remote sensing of water turbidity. Hydrological Sciences-Bulletin-des Sciences Hydrologiques, 25, 4, 12/1980

Ramakrishna B, C. Hang , B. Trou, J. Henquhemile. 2007. Chesapeake Bay water quality monitoring using satellite imagery. International Journal of High Speed Electronics & Systems [serial online]. December 2007;17 (4):681-688. Available from: Academic Search Premier, Ipswich, MA. Accessed November 9, 2011.

Rundquist, D.C. L.Han, J.F. Schalles, and J.S. Peake. 1996. Remote measurement of algal chlorophyll in surface waters: The case for the first derivative of reflectance near 690 nm.

Sun, D. , Y. Li, Q. Wang, C. Le, C.Huang, K.Shi. 2011. Development of optical criteria to discriminate various types of highly turbid lake waters. Hydrobiologia 669:83-104.